CERN HEALTH PHYSICS
DI/HP/28/Rev.

17 April, 1964

RADIATION DOSIMETRY FOR PROTECTION PURPOSES NEAR HIGH-ENERGY PARTICLE ACCELERATORS*)

by

J. Baarli and A.H. Sullivan

CERN, Geneva

* * *

ABSTRACT

The basic interactions occurring when very high-energy radiation passes through matter are briefly reviewed. It is concluded that the dosimetry near high-energy accelerators involves the measurements of a mixed field composed of proton, neutron, pion and gamma radiation as well as electrons and muons, all covering a very wide energy range.

The methods of measuring the rem dose in these radiation fields, using existing instrumentation, falls into two categories according to the dose-rate. Above 10 mrem/h, the tissue-equivalent ionization chamber in combination with a parallel plate chamber for quality factor measurements can be used. At lower dose-rates the sensitivity of these chambers limits their use and a system of six different instruments is required. This system enables the evaluation of the contribution to the total dose from slow and fast neutrons, high-energy particles and gamma rays.

Results of measurements using both these systems are presented for measurements in beams and behind shields of the CERN 600 MeV Synchro-cyclotron and the 28 GeV Proton Synchrotron. Behind thick shields in experimental regions of the PS machine, 11-22% of the total rem dose is caused by slow neutrons, 50-76% by fast neutrons, 2-25% by high-energy radiation, and 2-20% by gamma radiation.

---

*) Invited paper presented at the Physical Society Symposium on Neutron Dosimetry for Radiological Purposes, London, 24 January 1964.

INTRODUCTION

The dosimetry of very high-energy radiation has not been studied in any great detail until recently, when it has become necessary to judge radiation hazard near high-energy accelerators. Such accelerators are now in regular use for the study of elementary particle physics and approach a state where high-energy radio-biology is becoming feasible. The interest in this field is greatly stimulated by the possibility of space travel and the associated hazard from cosmic rays.

1. INTERACTION OF HIGH-ENERGY RADIATION WITH MATTER

The difficulty in applying conventional methods of dosimetry to very high-energy radiation arises from the differences in the interactions with matter; also high local energy deposition and high linear energy transfer (L.E.T.) values are associated with products from nuclear interactions. The measurement problem is further complicated by the presence of a wide variety and great energy range of secondary radiation accompanying the high-energy particle radiation.

Existing accelerators produce primary beams of protons up to 30 GeV. These protons are able to create particles such as those listed in Table 1[1]. Fortunately, in beams or behind shields many of these particles are not important for dosimetry because of their low production cross-section and short lifetime. The dosimetry problem arises mainly from high-energy protons, neutrons, pions and gamma rays as well as from electrons and muons.

The energy loss suffered by high-energy charged particles passing through matter occurs from ionization, and from nuclear and electromagnetic interaction. The primary ionization varies with energy, decreases when energy rises, reaches a minimum and rises again at very high energy on account of relativistic field distortion. For protons passing through tissue, the rate of energy loss can

have values between 100 keV/μ (in the Bragg peak region) down to 0.2 keV/μ at minimum ionization. Other charged particles behave similarly.

Table 2 shows the minimum rate of energy loss and the corresponding energy for the most common charged particles.

The problem of estimating the average specific ionization from rate of energy loss due to ionization requires knowledge of the energy dissipation in tissue by the particle itself and by its long-range secondaries. If a minimum ionizing electron enters the human body, it will be absorbed within 500 mg/cm^2. A rapidly increasing rate of energy loss, and consequently specific ionization will be found as the electron penetrates to this depth; when the energy is reduced to 1 keV, the value is about 12 keV/μ. On the other hand, if a proton of 2.5 GeV enters the body, it will only lose about 60 MeV by ionization and the rate of energy loss will hardly vary. However, a great part of this 60 MeV will have been lost as kinetic energy of secondary electrons. The average L.E.T. will therefore not be substantially different from that of low-energy electrons.

In addition to the ionization from the charged particles, nuclear interactions from charged and uncharged particles have also to be considered. These reactions can vary from more direct nuclear processes in which only a few particles from the excited nucleus take part to reactions in which the whole nucleus disintegrates emitting a large variety of particles and nuclear fragments (spallation). The cross-section for the more direct processes rises from a threshold to a maximum value and then decreases slowly to an approximative constant value which is reached between 150 and 250 MeV. These reactions involve local energy dissipation of the order of 10 MeV per emitted nucleon and are a source of low-energy secondary particles.

The cross-section for the spallation reaction rises slowly with energy up to several hundred MeV, and remains then nearly constant. The amount of energy dissipated locally in this case is very high. Apart from escaping neutrons, almost all the available energy contributes to the local dose. The total cross-section for the nuclear interactions is of the same order of magnitude as the geometrical size of the nucleus. The energy lost per unit path length by very high-energy charged particles when passing through matter is approximately equally divided between primary ionization and nuclear interactions.

2. HIGH-ENERGY RADIATION NEAR ACCELERATORS

The dosimetry problem near high-energy accelerators can be divided into two parts: in beams and behind shields. Pure beams of mono-energetic particles of very high energy are made by extracting protons from the vacuum chamber of accelerators. At CERN, a 600 MeV proton beam of an intensity of 10^5 to 10^{11} p/sec is available from the synchro-cyclotron, and arrangements have recently been made to extract the 28 GeV protons from the proton synchrotron. All other beams are made by exposing an internal target to the high-energy proton beam and selecting particle type and momenta using emission angle, and magnetic and electrostatic separators. These secondary beams are generally composed of several types of particles, due to particle decay. Typical examples are the K-beam of the CERN PS machine produced by 18.3 GeV protons. This beam at 100 milliradians contains at a momentum of 1.5 GeV/c more than 99% of $\pi^- + \mu^- + e^-$ with 0.4% K^- particles. The number of particles observed over an area of 2-3 cm^2 is around 1.7 x $10^5 \pi$ per 10^{10} protons accelerated [2]. Other beams are the scattered-out proton beam at 27 GeV which has an intensity of about 10^5 p/burst over 25 cm^2.

The usual secondary beams produced by the SC machine are, amongst others, a neutron beam of around 10^8 particles/sec of about 20 cm in diameter, and beams of pions and muons from 10^4 to 10^6 particles/sec. The beams are seldom pure and are contaminated with neutrons, pions, muons and often with a considerable quantity of electrons.

Besides the radiation in the actual beams, several regions behind shields are of interest for dosimetry measurements. Here the radiation is usually a mixture covering a wide energy range greatly depending on shielding thickness. Shielding studies for very high-energy radiation show that the high-energy flux densities increase with penetration depths up to 20 to 150 g/cm^2 by factors as high as 10, after which the intensity decreases with a mean free path according to the geometrical size of the nucleus [3]. This attenuation of the primary high-energy radiation produces secondary radiation of lower energies that comes into equilibrium with the beam. At large shielding thicknesses, the secondary radiation contributes the major part of the dose.

3. PRINCIPLES OF HIGH-ENERGY RADIATION DOSIMETRY

To make a complete measurement of the radiation dose equivalent (D.E.) for protection purposes, qualities like absorbed dose, quality factor (Q.F.) and build-up factor need to be estimated.

The methods of dosimetry at CERN have been based on these general principles. The only other approach would be to provide a complete knowledge of the radiation types and spectra and use the knowledge about the interactions to calculate the dose. The lack of any formal method of measuring dose within its definition has made it necessary to adopt the tissue equivalent ionization chamber reading as a measurement of absorbed dose independent of radiation type and energy. It has not been possible to check this arbitrarily

chosen definition of dose for all radiation. The response of the chamber however is satisfactory to fast neutrons, gamma rays and primary ionization of charged particles [4].

Having defined the dose in instrument reading, depth dose distribution is readily measured using water absorbers to resemble tissue.

The third quantity necessary is the Q.F. and its variation with depth. This quantity should not be confused with the R.B.E. which is defined entirely by biological effects. The Q.F. depends only on the average L.E.T. and is supposed to cover the most critical effects of radiation and is therefore considered to express the maximum R.B.E. of the radiation in question. The relationship between L.E.T. and Q.F. is shown in Fig. 1.

Attempts have been made to estimate Q.F. by measuring a recombination index using a parallel plate ionization chamber filled at high pressure with a tissue equivalent gas [5]. The functioning of this chamber is explained by columnar recombination which is a function of specific ionization and hence of Q.F. It has been found that the measured index of recombination is proportional to the Q.F. and that this response is independent of dose-rate and angular distribution of the radiation. Furthermore it averages the Q.F. for a mixture of radiation.

The method outlined for measuring dose and dose equivalent is only practical when the dose-rate exceeds the maximum permissible levels, since the present sensitivity of the instrumentation involved limits the accurary at low levels.

For measurements behind shields where the radiation levels are well below tolerance, conventional health physics instruments have to be used. A system of instruments is therefore employed from which the contribution to the dose of the various types and energy ranges are determined separately.

The system used for routine measurements is shown in Table 3. Behind thick shields, depth dose determinations are not necessary since the radiation can be assumed to be in equilibrium, which will not be significantly disturbed by the presence of the body.

The simplest approach to a dose estimation from this system is to use the reading of a tissue equivalent ionization chamber in combination with a CO_2 or Air chamber to estimate the gamma and neutron dose separately [6]. Primary ionization of charged particles from electrons, protons, pions or muons, etc., is then included in the apparent gamma dose.

Having established these two components, Q.F. of 1 and 10 could be applied to get a first order approximation of the dose equivalent. If the neutron component includes high-energy particles, a more accurate estimate of the dose can be made by measuring the neutrons and high-energy component separately.

Thermal neutrons are measured by using a BF_3 chamber calibrated in mrem. Fast neutron flux is measured independently of energy up to 14 MeV using the Long Counter or by foil activation in a moderator [7]. The neutron energy flux is measured by a proton recoil counter [8]. Combining these two readings, the average energy of the neutrons is obtained, enabling the flux to be converted to rem dose using the recommended relation [9].

High-energy strong interacting particle flux is measured by activation of carbon in plastic phosphors [6]. The cross-section of this reaction is such that a relatively energy-independent flux measurement from about 20 MeV and upwards can be made. To convert this flux to dose, calculated values have to be used. In the following, some preliminary measurements of these values are repeated.

This system of instruments is thought to give the best analysis of the radiation within the limits of available instrumentation. There exist gaps such as the epithermal and lower energy neutrons and the range between 14 and 20 MeV which is not completely covered by this system. The system tends however to overestimate the dose as the detectors respond to a small extent to radiation other than the radiation to which the readings are attributed.

4. DOSIMETRY OF HIGH-ENERGY BEAMS

The principles of dosimetry outlined above, have been used to measure beams and radiation fields behind shields at CERN. The dosimetry of beams has been limited to those with sufficient intensity. Results have been obtained for the 600 MeV proton beam and for secondary beams scattered out at 0°, 18°, 36° and 56° from the 600 MeV synchro-cyclotron. A larger number of measurements have been carried out behind shields near both accelerators.

The absorbed dose-rate in the 600 MeV proton beam was measured with the T.E. chamber. In order to give the readings a meaning in the strongly varying beam profile, they were related to the average flux passing through the chamber. Measurement of the beam profile was made with a 0.6 cm^3 ionization chamber and these measurements were checked by exposing C^{11} phosphors of 44 and 125 mm in diameter.

The results are shown in Fig. 2, where the fraction of the beam as a function of the diameter is shown. The results show that the intensity measured by the ionization chamber coincideswith the flux density measurements. The total beam was monitored by a secondary emission chamber absolutely calibrated using the Al^{27} (p5n5p) F^{18} reaction [10].

Build-up measurements were made with a water phantom in combination with a T.E. chamber where the diameter of the cylindrical phantom was varied.

Similar measurements were also made in secondary beams using an internal Be target. The results are shown in Table 4 which shows the estimated contributions from the different components of the radiation and the measured Q.F. for the different beams. At 0°, the proton energy was 400 MeV, at the other angles 580 MeV. The energy stated is calculated from the kinetics assuming elastic collision in the target. The spectral distribution of the neutrons is largely uncertain but the energy decreases with increasing angle of observation. All the measurements refer to a depth of about 1 g/cm^2. The separate contributions to the dose from gamma rays, proton recoil neutrons, high-energy neutral and charged particles by the selected detectors. These estimates were made primarily to obtain some first order information of the dose from the high-energy neutral component and then relate this to flux.

The experimentally determined Q.F.s are of particular interest in this table. The same value of Q.F. within experimental errors is found for all 4 neutron beams. The Q.F. of the proton beam, however, is considerably smaller.

Table 5 shows the dose-rates measured in the same beams at the depth of maximum build-up. Compared to Table 4, the over-all measured Q.F.s have lower values after this depth of penetration. It should also be noted that the build-up and the depth at which it occurs cannot be neglected in a measurement of the dose in a neutral beam.

Table 6 shows the D.E. for the various beams and the corresponding measured flux densities of particles above 20 MeV. Based on the information given in Tables 4 and 5, the flux per mrem hour of the total dose as well as of the high-energy neutrons at maximum build-up is shown. The flux per mrem per hour at the surface is included for comparison.

The errors in the figures are of the order of 30%.

The figures listed in the fifth column show the degree to which dose is found proportional to flux independent of particle type and energy. The lower value stated for the protons is due to the primary ionization of this particle. From the results in the table it is possible to estimate a figure of 10 to 20 high-energy particles per cm^2/sec equivalent to 1 mrem per hour when build-up and Q.F. at maximum build-up are considered and secondaries are measured independently. A number greater than 7 particles cm^2/sec is found when the secondaries are included. This figure which refers to a pure beam can be compared with 4 n/cm^2/sec that has been submitted from the M.R.C. to the I.C.R.P. [9].

To convert routine high-energy flux measurements to dose according to the scheme of dose estimation, a figure of 10 n/cm^2/sec equivalent to 1 mrem/hour is applied. The associated secondaries are determined separately, as described above. This figure will ensure an overestimate when making routine measurements. It will, however, resolve in an underestimation for the dose from protons, but this is compensated for by the primary ionization dose already measured separately by ionization chambers.

5. DOSIMETRY MEASUREMENTS BEHIND SHIELDS

The method of dosimetry behind shields has been described above. A selection of some results at different locations and under varying conditions is shown in Table 7.

These measurements include dose-rates from 0.25 mrem/hour up to 14 mrem/hour. The distribution of the dose between the various radiation types and energies has been calculated. The results are shown in Table 8 for four different locations near the CERN PS machine.

The North Experimental hall is located on the inside of the circulating beam, and the South Experimental hall on the outside. The bridge is a thin concrete shield (1.80 m) above the target area. The μ region is in the direction of the tangent to the target being used.

It can be seen that the major fraction of the dose is due to fast neutrons; thermal neutrons, gamma rays and high-energy particle radiation together contribute approximately as much as the fast neutrons. The dose seems to be distributed in about the same way for any regions near the accelerator with the exception of a typical μ region where the gamma radiation (charged particles) is the principal radiation. The observed apparent quality factor does not seem to vary very much in the different regions.

If a single detector is required, the T.E. chamber will give the best rem dose estimation. Assuming a Q.F. of 10, the maximum over-estimation of dose-rate will be about 2. However, this chamber is limited in sensitivity, and dose-rates less than 0.1 mrad/hour are not easily measured. At low dose-rates, the Long counter and the proton recoil counter seem to give the best results. In this way, the dose can be obtained by simply multiplying the measurements by a factor of 2.

The authors would like to express their thanks to Dr. S. Charalambus, Dr. A. Rindi, J. Coleman and C. Raffnsøe, for their assistance with the measurements.

REFERENCES

1) B.P. Gregory, Proceedings of the 1962 International Conference on High-Energy Physics, CERN, page 783.

2) CERN Proton Synchrotron User's Handbook Vol.1, L 49 P 5, 1962.

3) J. Baarli, K. Goebel and A.H. Sullivan, "An experimental study of the penetration of 10 and 19.2 GeV proton radiation in steel", DI/HP/15, 1963.

4) H.H. Rossi, G.J. Hine and G.L. Brownell, Academic Press, p. 882 (1958).

5) A.H. Sullivan and J. Baarli, "An ionization chamber for the estimation of the biological effectiveness of radiation", CERN Report 63-17, 1963.

6) J. Baarli, K. Goebel and A.H. Sullivan, "The calibration of health physics instruments used to measure high-energy radiation", "Health Physics", Vol.9, pp.1057-67, 1963.

7) L.D. Stephens and H. Aceto, Jr., I.A.E.A. "A neutron dosimetry", page 535.

8) B. Moyer, Nucleonics 10, 5, (1962).

9) Imperial College Code of Radiation.

10) D. Harting, J.C. Kluyver and A. Kusumegi, "Absolute intensity measurements on the external proton beam of the CERN Synchro-cyclotron. CERN Report 60-17, 1960.

QF AS A FUNCTION OF LET

Fig. 1

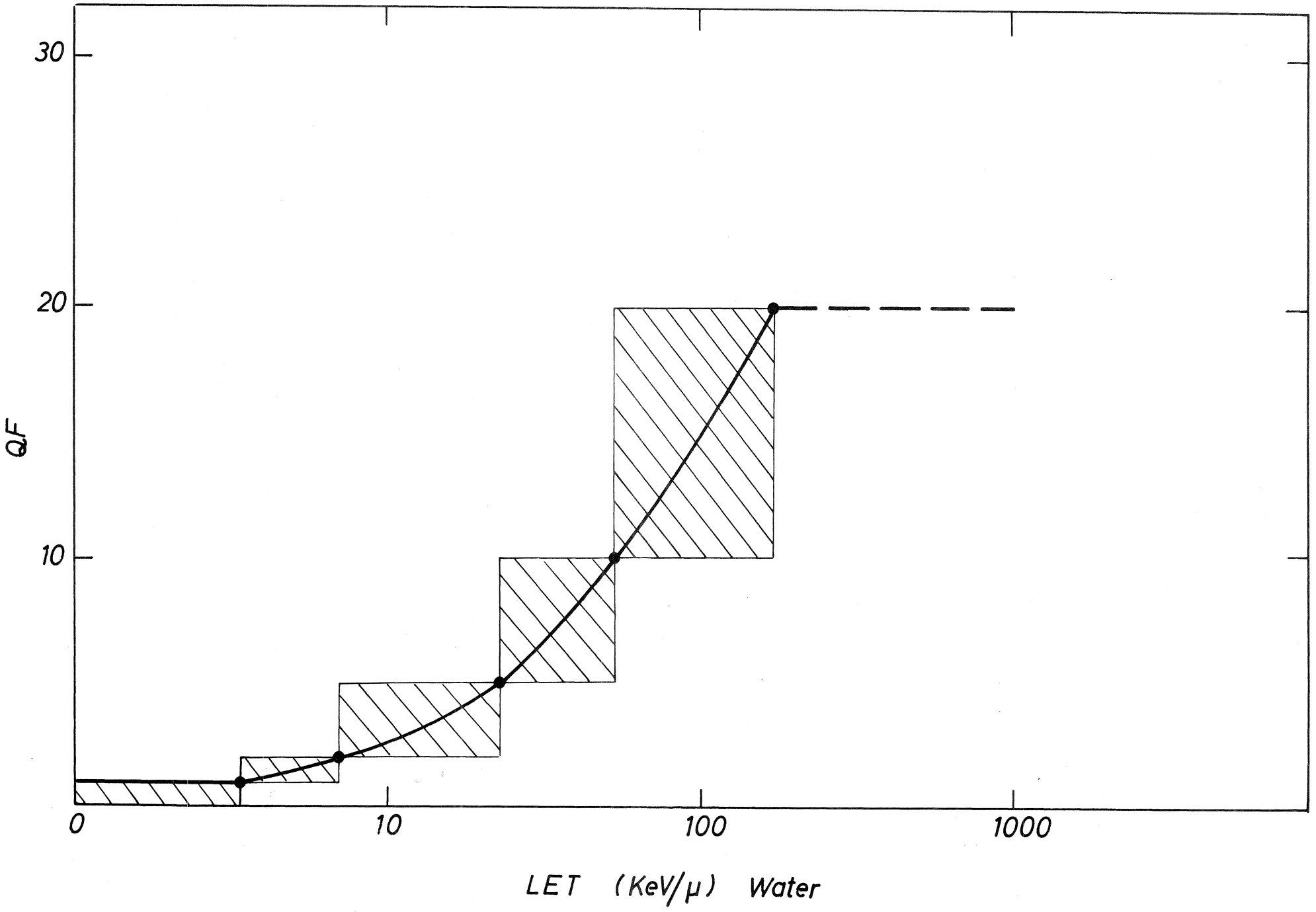

FRACTION OF BEAM THROUGH CIRCLE OF VARIOUS RADII

SC 600 MeV proton beam

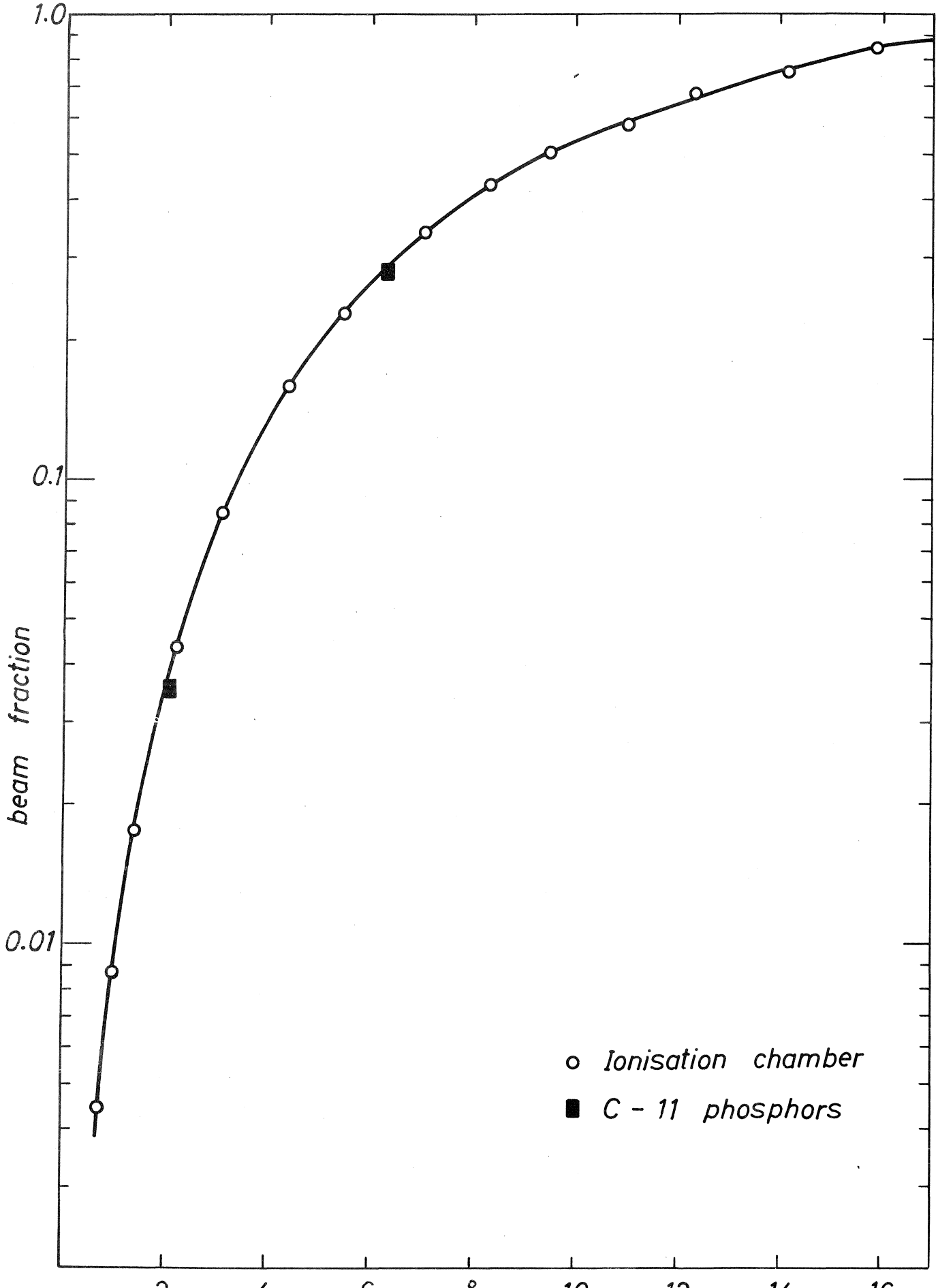

ADM/526

Fig. 2

Table 1

Elementary particles

Particle		Electric charge	Mass in MeV	Spin	Strangeness	Mean lifetime in seconds	Common disintegration products	Antiparticle
Baryons								
Ξ^-	(xi minus)	- e	1321	½?	- 2	1.2×10^{-10}	$\pi^- + \Lambda$	$\bar{\Xi}^+$ (antixi plus)
Ξ^o	(xi zero)	0	~1311	½?	- 2	$\sim 2\times10^{-10}$	$\pi^o + \Lambda$	$\bar{\Xi}^o$ (antixi zero)
Σ^-	(sigma minus)	- e	1196	½	- 1	1.6×10^{-10}	$\pi^- + n$	$\bar{\Sigma}^+$ (antisigma plus)
Σ^o	(sigma zero)	0	1192	½	- 1	$\approx 10^{-20}$	$\gamma + \Lambda$	$\bar{\Sigma}^o$ (antisigma zero)
Σ^+	(sigma plus)	+ e	1189	½	- 1	0.8×10^{-10}	or $\pi^+ + n$ / $\pi^o + p$	$\bar{\Sigma}^-$ (antisigma minus)
Λ	(lambda)	0	1115	½	- 1	2.5×10^{-10}	or $\pi^- + p$ / $\pi^o + n$	$\bar{\Lambda}$ (antilambda)
n	(neutron)	0	940	½	0	1.0×10^{3}	$e^- + \bar{\nu}_e + p$	$\bar{n}$ (antineutron)
p	(proton)	+ e	938	½	0	stable	-	$\bar{p}$ (antiproton)
Bosons								
K^o	(K zero)	0	498	0	+ 1	10^{-10}	$\pi^+ + \pi^-$	$\bar{K}^o$ (anti-K zero)
K^+	(K plus)	+ e	494	0	+ 1	1.2×10^{-8}	or $\mu^+ + \nu_e$ / $\pi^+ + \pi^o$	K^- (K minus)
π^+	(pi plus)	+ e	140	0	0	2.5×10^{-8}	$\mu^+ + \nu_\mu$	π^- (pi minus)
π^o	(pi zero)	0	135	0	0	1.01×10^{-16}	$\gamma + \gamma$	itself
γ	(photon)	0	0	1	0	stable	-	itself
Leptons								
μ^-	(mu minus)	- e	106	½	undefined	2.26×10^{-6}	$e^- + \nu_e + \bar{\nu}_\mu$	μ^+ (mu plus)
e^-	(electron)	- e	0.511	½	undefined	stable	-	e^+ (positron)
ν_e	(neutrino)	0	0	½	undefined	stable	-	$\bar{\nu}_e$ (antineutrino)
ν_μ	(neutrino)	0	0	½	undefined	stable	-	$\bar{\nu}_\mu$ (antineutrino)

Table 2

Minimum rate of ionization energy loss for protons, pions, muons and electrons

Particle	Energy	Rate of Energy Loss
Proton	2.5 GeV	0.20 keV/μ
Pion	370 MeV	0.20 keV/μ
Muon	200 MeV	0.19 keV/μ
Electron	1 MeV	0.19 keV/μ

Table 3

Survey instruments for high-energy radiation monitoring.

Radiation	Energy Range	Instruments	Quantities Determined
High-energy particle	E > 20 MeV	Induced Carbon-11 in phosphors	Flux density
Fast neutron	100 keV < E < 15 MeV	Long counter	Flux density
Fast neutron	100 keV < E < 15 MeV	Moderated activation of Indium foil	Flux density
Fast neutron	100 keV < E < 15 MeV	Proton recoil counter	Energy flux
Thermal neutron	0.25 eV	BF_3 chambers	Dose
Gamma and direct ionizing radiation	E > 100 keV	Twin ionization chambers	Gamma dose (+ primary ionization)

Table 4

Absorbed dose under 1 g/cm^2 in high-energy beams.

Beams Neutron Energy (Scattered)	Dose-rates rad/h					Quality Factor
	Total	Charged Particle	Neutral Particle	Gamma Radiation	Fast Neutron	
400 MeV	3.03	< 0.06	3.03	< 0.37	-	3.5 ± 0.7
525 "	2.06	0.23	1.83	< 0.36	0.10	2.6 ± 0.6
360 "	1.20	0.09	1.11	< 0.15	0.26	2.4 ± 0.6
180 "	1.03	0.18	0.85	< 0.11	0.19	2.8 ± 0.5
Protons 600 MeV	-	100%	-	-	-	1.2 ± 0.3

Table 5

Dose at maximum build-up in high-energy beams.

Beams Neutron Energy (Scattered)	Total Dose rad/h	Depth g/cm^2	Proton Recoil Contribution rad/h	Build-up	Quality Factor
400 MeV	7.5	15 - 20	-	2.50	2.0 ± 0.5
525 "	4.6	16 - 20	0.36	2.50	1.7 ± 0.5
360 "	2.2	12 - 15	0.40	2.00	2.0 ± 0.5
180 "	1.6	8 - 12	0.18	1.85	2.4 ± 0.5
Protons 600 MeV	-	10 - 15	-	1.2	1.2 ± 0.3

Table 6

Relation between high-energy particle flux and dose.

Beams Neutron Energy (Scattered)	Dose Rate rem/h	Flux Density > 20 MeV	Flux per mrem/h Total Dose	Flux per mrem/h High-Energy Particle Dose	Flux per mrem/h under 1 g/cm^2
400 MeV	15	2.15×10^5	14	16	20
525 "	7.8	1.04×10^5	13	16	20
360 "	4.5	4.4×10^4	10	24	15
180 "	3.8	2.8×10^4	7	16	10
Protons 600 MeV	-	-	6.3	6.3	7.5

Table 7

Analyses of survey results near the CERN SC and PS machines.

Location of Measurements	High Energy Part. Carbon-11		Fast Neutrons			Gamma Dose	Thermal Neutrons	Total Dose	T.E. Dose	Apparent Quality Factor
	Flux part/cm²/sec	Dose mrem/h	Flux n/cm²/sec	Average $\bar{E}$ MeV	Dose mrem/h	mrad/h	mrem/h	mrem/h	mrad/h	
At large distances	< 0.8	< 0.08	25	0.6	2.5	0.02	-	2.6	0.9	2.9
while the 600 MeV	< 1.2	< 0.12	1	1.1	0.1	0.03	-	0.25	0.04	6.2
SC external proton	2.0	0.2	48	1.3	6.9	0.3	-	7.4	0.62	12
beam is operating	< 0.8	< 0.08	22	0.9	3.0	0.5	-	3.1	0.28	11
Near SC neutron	< 0.8	< 0.08	3.8	1.5	0.54	0.06	-	0.7	0.07	10
hall while inter-	1.5	0.15	5.4	0.9	0.72	0.03	-	0.9	0.07	13
nal target is in	3.3	0.33	7.3	4.4	1.05	0.42	-	1.8	0.5	3.6
operation	15.6	1.6	7.5	11.6	1.1	0.83	-	3.6	0.9	4
Near PS target	5.2	0.52	26.2	2.8	3.9	0.36	0.9	4.32	1.0	4.3
region (bridge)	22.8	2.28	64	3.4	9.2	1.26	1.85	15.59	3.8	4.1
	27.0	2.7	39	4.9	5.6	0.85	1.7	11.3	1.9	6.0
	4.4	0.44	22.8	1.9	3.3	0.31	0.69	4.74	0.8	5.9
Near PS north hall	< 0.8	< 0.08	2.2	1.1	0.3	0.05	0.12	0.54	0.04	13
when internal tar-	< 0.8	< 0.08	3.0	0.7	0.4	0.05	0.15	0.68	0.06	11
get in operation	< 0.8	< 0.08	4.3	1.0	0.6	0.04	0.16	0.87	0.11	8
	< 0.8	< 0.08	3.7	1.2	0.53	0.01	0.12	0.71	0.05	14

Table 8

Distribution of the radiation dose near the CERN PS accelerator

	High-energy particles	Fast neutrons	Gamma radiation	Thermal neutrons	Apparent quality factors
PS North Experimental Hall	2 - 14 %	55 - 76 %	2 - 9 %	14 - 22 %	4.4 - 14
PS South Experimental Hall	10 - 14 %	54 - 62 %	7 - 19 %	12 - 22 %	2.8 - 5.3
PS Bridge	9 - 25 %	50 - 70 %	6 - 9 %	11 - 16 %	3.8 - 59
PS muon region	1 %	15 %	83 %	1 %	1.2